

# Influence of Signal Stationarity on Digital Stochastic Measurement Implementation

Platon Sovilj, Vladimir Vujičić, Nebojša Pjevalica, Dragan Pejić, Marjan Urekar, and Ivan Župunski

**Abstract**—The paper presents the influence of signal stationarity on digital stochastic measurement method implementation. The implementation method is based on stochastic voltage generators, analog adders, low resolution A/D converter, and multipliers and accumulators implemented by Field-Programmable Gate Array (FPGA). The characteristic of first implementations of digital stochastic measurement was the measurement of stationary signal harmonics over the constant measurement period. Later, digital stochastic measurement was extended and used also when it was necessary to measure time-series of non-stationary signal over the variable measurement time. The result of measurement is the set of harmonics, which is, in the case of non-stationary signals, the input for calculating digital values of signal in time domain. A theoretical approach to determine measurement uncertainty is presented and the accuracy trends with varying signal-to-noise ratio (SNR) are analyzed. Noisy brain potentials (spontaneous and non-spontaneous) are selected as an example of real non-stationary signal and its digital stochastic measurement is tested by simulations and experiments. Tests were performed without noise and with adding noise with SNR values of 10dB, 0dB and -10dB. The results of simulations and experiments are compared versus theory calculations, and comparison confirms the theory.

**Index Terms**—Digital measurements, stochastic measurements, measurement uncertainty, brain potentials.

Original Research Paper  
DOI: 10.7251/ELS1317045S

## NOMENCLATURE

$s$  – noisy signal measured after conditioning  
 $s_e$  – amplified input signal  
 $n$  – noise in signal at the input of digital block  
 $s_a$  – auxiliary signal (dithered base function)  
 $S_a$  – the root mean square (RMS) value of the auxiliary signal  
 $d_i$  – dithering signal  
 $p(d_i)$  – probability density function of  $d_i$  dithering signal  
 $\Delta_i$  – quantum of the uniform quantizer

$p(n)$  – probability density function of noise  $n$   
 $T$  – measurement subinterval  
 $f_0$  – fundamental frequency  
 $f_{adc}$  – sampling frequency of analog-to-digital (A/D) converter in digital stochastic measurement block  
 $R$  – input range  
 $N$  – number of samples within measurement subinterval  
 $N_h$  – number of harmonics measured by digital stochastic measurement block  
 $\Psi_e$  – result of A/D conversion of dithered signal  $s$   
 $\Psi_a$  – result of A/D conversion of dithered base function  
 $\Psi_{acosk}$  – result of A/D conversion of dithered cosine function with period  $\omega = 2\pi kf_0$   
 $\Psi_{asin k}$  – result of A/D conversion of dithered sine function with period  $\omega = 2\pi kf_0$   
 $\Psi$  – digital multiplier output  
 $\Psi_{cosk}$  – digital multiplier output for measuring cosine component of  $k$ th harmonic  
 $\Psi_{sin k}$  – digital multiplier output for measuring sine component of  $k$ th harmonic  
 $a_k$  – cosine Fourier coefficient of  $k$ th harmonic i.e. trigonometric polynomial cosine coefficient of order  $k$   
 $b_k$  – sine Fourier coefficient of  $k$ th harmonic i.e. trigonometric polynomial sine coefficient of order  $k$   
 $u(\bar{\Psi})$  – standard measurement uncertainty  
 $u$  – relative measurement uncertainty  
 $\sigma_\Psi^2$  – variance of digital multiplier output  
 $\sigma_d^2$  – deterministic variance  
 $\sigma_n^2$  – noise variance  
 $\sigma_r^2$  – random variance (noise induced)  
 $\sigma_e^2$  – variance due to quantization error and dither

## I. INTRODUCTION

ALL signals can be divided into either stationary or non-stationary categories. Non-stationary signals are not constant in their statistical parameters over time (i.e. its amplitude distribution and standard deviation are not the same over time). Stationary signals are constant in their statistical parameters over time. Stationary signals further can be divided into deterministic and random signals. Random signals are unpredictable in their frequency content and their amplitude level, but they still have relatively uniform statistical characteristics over time [1-2].

Advanced measurement instrumentation is based on digitizing hardware components. Measured signals are usually

Manuscript received 15 April 2013. Received in revised form 12 June 2013. Accepted for publication 13 June 2013.

This work was supported in part by the Ministry of Science and Technological Development of Republic of Serbia under research grant No. TR32019, and supported in part by the Provincial secretariat for science and technological development of Autonomous Province of Vojvodina (Republic of Serbia) under research grant No. 114-451-2723.

The authors are with the Faculty of Technical Sciences, University of Novi Sad, Novi Sad, Serbia (Corresponding author e-mail: platon@uns.ac.rs).

conditioned and time-continuous conditioned signals are sampled and converted into discrete digital variables. In the A/D conversion process, accuracy and speed are opposing requirements, and accurate measurements of low-level, noisy and distorted signals have been a challenging problem in the theory and practice of measurement science and technology.

A possibility for reliable operation of instruments with inherent random error has been researched since 1956 [3]. An inherent property of such an approach is a very simple hardware, which can operate very fast. It has been shown that adding a random uniform dither to an A/D converter input decouples measurement error from the input signal [4]. This dither also suppresses the measurement error due to both coarse A/D conversion and the external additive noise in the input signal.

Following this generic approach, several specific methods has been developed for measuring average DC inputs, AC inputs and/or distorted AC inputs. Several prototype and small-series commercial instruments has been realized and their measurement uncertainty can be extremely low [5-6]. These methods were named digital stochastic measurement methods and these instruments were named digital stochastic instruments.

The latest prototype instrument is a digital stochastic instrument for measurement of harmonics of mains voltage and current signals, reported in [7]. This instrument performs harmonic analyses for the DC component and up to 49 harmonics (both cosine and sine components) in each of seven different input channels. Its operation is based on stochastic A/D conversion and accumulation, with a hardware structure designed for harmonic measurements. The method and the predicted uncertainty for fifty harmonics are validated in [7] by simulation and experiments using sampling frequency of 250 kHz per channel.

In paper [8] digital stochastic measurement method is investigated for various types of stationary signal. The results demonstrated the ability of this method to be applied for measurements of harmonics of any stationary signal. After that, the question was if it was possible to extend the method for being used in measuring non-stationary signals? The research described in [9], lead to positive answer, so the method can be applied in measurement of biomedical signals, audio signals, video signals etc.

This paper describes the influence of signal stationarity on digital stochastic measurement implementation, and it is based on researching theoretical models of digital stochastic measurement of stationary and non-stationary signals and their consequences in the form of mathematical formulas, and on researching simulated measurement and real measurement of

brain potential as a non-stationary signal example.

## II. ANALYSYS OF METHOD

### A. Digital Stochastic Measurement and Signal Stationarity

Measurement system based on digital stochastic measurement can be divided into three blocks: conditioning block, digital stochastic measurement block and block for data processing, recording and presenting (Fig. 1).

The signal at the input of digital stochastic measurement block is the conditioned signal. The role of this conditioning can be amplification, linearization, level transition, filtering, galvanic isolation, various techniques for rejecting noise etc. In this paper the focus of analysis is the implementation of digital stochastic measurement, neglecting the non-linearity issues of the components consisting conditioning block. Hence, it is proposed that conditioned signal  $s$  is the sum of linearly amplified input signal  $s_e$  (which will be called just “amplified input signal” in further text) and the white noise  $n$  with uniform or Gaussian amplitude distribution:

$$s = s_e + n \quad (1)$$

Noise  $n$  is assumed to be the sum of all the noises which were not rejected before the digital stochastic measurement system. The sources of the noise can be the phenomenons inside the conditioning block, but also inside the conditioning block input interface, and inside the interface between conditioning block and digital stochastic measurement block. In this paper, we do not consider the nature of various noise sources and the phenomenons behind them, but focus on the general model of noise.

If short-time Fourier transform would be applied to signal  $s_e$  by window function of width equal to measurement subinterval  $T$ , resulting in Fourier coefficients  $a_i$  and  $b_i$ , then  $s_e$  can be presented as a trigonometric polynomial of the form:

$$s_e(t) = \frac{a_0}{2} + \sum_{n=1}^M a_n \cos n\omega_0 t + \sum_{n=1}^M b_n \sin n\omega_0 t, \quad 0 < t < T \quad (2)$$

In (2)  $\omega_0 = 2\pi/T$  and  $M$  is the order of trigonometric polynomial [7].

Concept of digital stochastic measurement compared with typical digital measurement is shown at Fig. 2. The outputs of digital measurement are digital values in time domain. Each digital value is actually digitized value of appropriate analog sample from the input and that is well known classical approach of digital measurement – sample by sample.

Instead of such approach, the outputs of digital stochastic measurement are Fourier coefficients  $a_i$  and  $b_i$ . Each Fourier coefficients is the function of all analog samples from the input over the measurement subinterval. Hence, this method is not based on “sample by sample” approach, but it is an

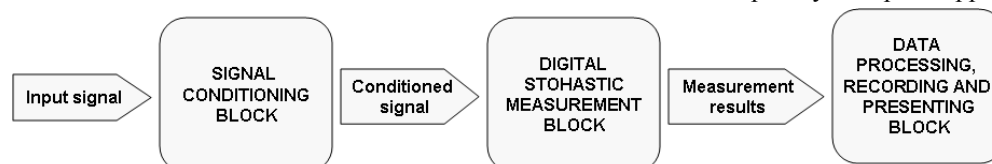


Fig. 1. Measurement system based on digital stochastic measurement.

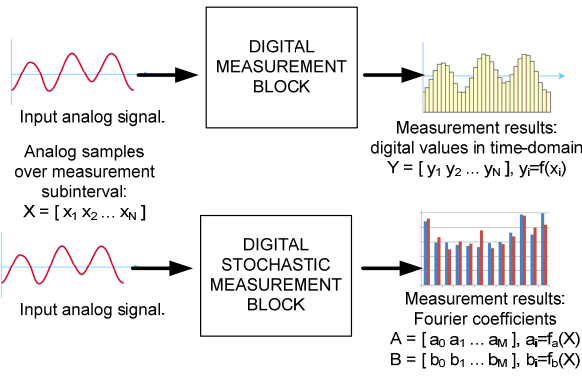


Fig. 2. Typical digital measurement versus digital stochastic measurement.

interval-based method.

At first sight it can be concluded that digital stochastic measurement is convenient only for measuring harmonics of stationary signals. But, it can be also used for measuring non-stationary signals. The result of measurement is the set of harmonics, which can be the input for calculating digital values of signal in time domain. This calculation can be simple the calculation of trigonometrial polynomial (2) at each time instant over the measurement subinterval  $T$ , or it can be Inverse Fast Fourier Transform (IFFT) over the measurement subinterval  $T$  which is faster method. Hence, the final results are a) the set of harmonics of the signal over the measurement subinterval  $T$  and b) time-series of the signal over the measurement subinterval  $T$  (Fig. 3).

This method has not to be limited to measurement subinterval  $T$ . If we want to measure the signal over the longer measurement interval  $[0, T_m]$ , where  $T_m = m \cdot T$ , than it is possible to divide original measurement interval to measurement subintervals  $[0, T]$ ,  $[T, 2T]$ , ...,  $[(m-1)T, mT]$ . Measurement and calculation can be executed for the first subinterval, and subsequently, subinterval by subinterval, signal values in time-domain can be reconstructed over the whole measurement interval  $[0, T_m]$ .

### B. Measurement of One Fourier Coefficient

The instrument presented in [7, 8] is designed to measure harmonics of mains voltages and currents, but its concept can be applied to measurement of harmonics of any signal that can be presented as (2). Therefore its concept is the base for conceptual block diagram of digital stochastic measurement of one Fourier coefficient of the amplified input signal. (Fig. 4)

Auxiliary signal  $s_a$  is a dithered base (cosine or sine) function. That is,  $s_a = R \cos k\omega_0 t$  for measuring  $k$ th cosine Fourier coefficient, or  $s_a = R \sin k\omega_0 t$  for measuring  $k$ th sine

Fourier coefficient.

Similarly to [7] the conceptual block diagram can be implemented as in Fig. 5 so  $s_a$  is not to be a measured signal, but a dithered sine or cosine function generated in advance and stored in the memory.

$d_1$  and  $d_2$  are generated dithering signals and they satisfy the following conditions that limit their amplitude and define their probability density function:

$$0 \leq |d_i| \leq \frac{\Delta_i}{2} \quad (3)$$

$$p(d_i) = \frac{1}{\Delta_i}, \text{ for } i = 1, 2 \quad (4)$$

Sampled values of conditioned signal  $s$  and auxiliary signal  $s_a$  at every time instant within the measurement subinterval ( $T$ ) are  $\psi_e$  and  $\psi_a$ , respectively. The measured value  $\psi$  (multiplier output) differs from the input signals' product by the measurement error  $e$ , which includes effect of quantization within A/D converter and the introduced dither:

$$\Psi = \Psi_e \cdot \Psi_a = s \cdot s_a + e \quad (5)$$

As the measured conditioned signal consists of the amplified input signal and the noise, then:

$$\Psi = s_e \cdot s_a + n \cdot s_a + e \quad (6)$$

The first term of the multiplier output is the signal that is to be measured and the second term is caused by noise. The three terms in (6) are statistically independent, and average  $\bar{\Psi}$  is the sum of their average values.

The average value of the third term in (6) is zero, as shown in [10] and does not affect the average value of the expected output  $\bar{\Psi}$  over the measurement subinterval. A finite input range of  $\pm R$  of digital stochastic measurement block defines the boundary of the average noise integration. Therefore the remaining two terms in the average value are [5]:

$$\bar{\Psi} = \frac{1}{T} \int_0^T s_e \cdot s_a dt + \left( \int_{-R}^R n \cdot p(n) dn \right) \frac{1}{T} \int_0^T s_a dt \quad (7)$$

If we assume that the noise has a Gaussian unbiased nature, its average value is zero so that the second term in (7) becomes zero, and then:

$$\bar{\Psi} = \frac{1}{T} \int_0^T s_e \cdot s_a dt. \quad (8)$$

In digital measurements, for  $N$  samples of the conditioned signal over the subinterval  $[0, T]$ , the average value is [7]:

$$\bar{\Psi} = \frac{1}{N} \sum_{k=1}^N \Psi_k \quad (9)$$

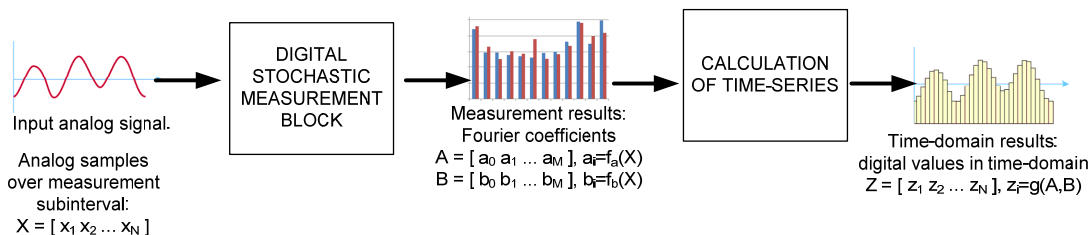


Fig. 3. Concept of measuring signal in time-domain by digital stochastic measurement over one measurement subinterval.

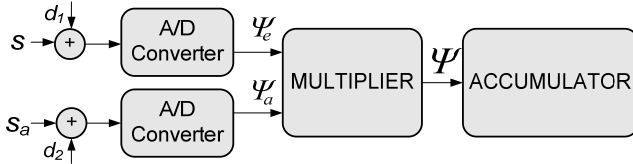


Fig. 4. Conceptual block diagram of digital stochastic measurement of one Fourier coefficient of amplified input signal. The accumulator output is used for calculation of the coefficient.

Summing of samples during the measurement subinterval is done by the accumulator and this sum is the output of the accumulator (Fig. 5). This output can be processed by microprocessor which divide the accumulator output by the number of samples  $N$ , and also calculates each sine (or cosine) component of the  $k$ th harmonic of the output as in [7] (subscripts  $sin k$  and  $cos k$  indicates that  $k$ th sine and  $k$ th cosine Fourier coefficient is measured) :

$$a_k = \frac{2\bar{\Psi}_{\cos k}}{R}, \quad b_k = \frac{2\bar{\Psi}_{\sin k}}{R} \quad (10)$$

### C. Measurement of Predefined Set of Harmonics

The concept of measuring one Fourier coefficient of the amplified input signal can be extended as in Fig. 6, which presents more complex conceptual block-diagram for measuring predefined set of harmonics of conditioned signal at the input of digital stochastic measurement block (DSMB). Beside DC component, predefined set can include all the harmonics which are interested for the signal analysis. Memory gives dithered base functions for each sine and

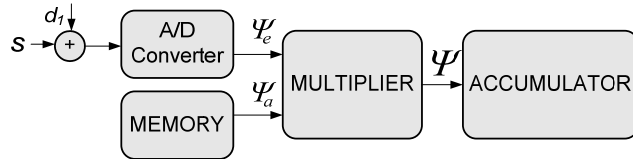


Fig. 5. Improved conceptual block diagram of digital stochastic measurement of one Fourier coefficient of amplified EEG signal. Instead of using two A/D converters, digital samples of the dithered base function are stored in memory.

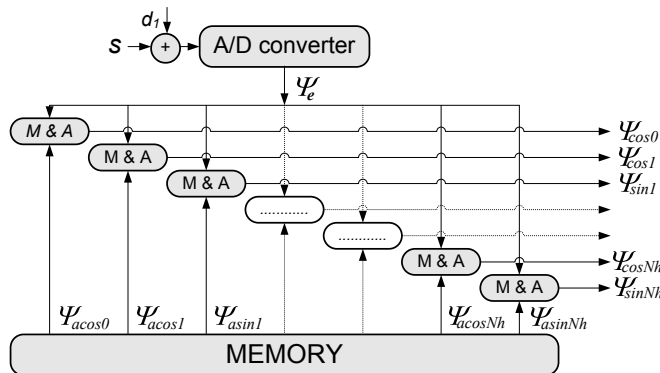


Fig. 6. Conceptual block diagram of digital stochastic measurement of predefined set of signal harmonics. Each element marked with M&A is consisted of one multiplier and one accumulator. Each output should be divided by  $N$  for calculating appropriate, which is necessary for further calculation of Fourier coefficients.

cosine component, and each sine and cosine component requires one digital multiplier and digital accumulator. Therefore, if the system should measure DC component and  $N_h$  harmonics this structure requires  $2N_h+1$  multipliers and  $2N_h+1$  accumulators.

At first sight, block diagram from Fig. 6 seems to require complex hardware structure but its hardware implementation can be relatively simple by using FPGA (it is described in more details in section dedicated to experiments).

### D. Measurement Uncertainty

In [7] output and relative measurement uncertainty were analyzed, and calculations of variance of multiplier output lead to determining variance of the average accumulator output and the relative measurement uncertainty. In digital stochastic measurement block the variance of the multiplier output is also consisted of deterministic variance, random variance and error (stochastic-related) variance. These parts are uncorrelated, hence the total variance of  $\Psi$  is [7]:

$$\sigma_{\Psi}^2 = \sigma_d^2 + \sigma_r^2 + \sigma_e^2 \quad (11)$$

Deterministic variance  $\sigma_d^2$ , according to [7], is defined as:

$$\sigma_d^2 = \frac{1}{T} \int_0^T (s_e s_a)^2 dt - \left( \frac{1}{T} \int_0^T s_e s_a dt \right)^2 \quad (12)$$

However the deterministic variance  $\sigma_d^2$  is the property of the signal and is not to be included to the measurement uncertainty [7]. Random variance and error (stochastic-related) variance,  $\sigma_r^2$  and  $\sigma_e^2$ , satisfy the central limit theorem [11] and variances of their average values depend on the number of samples  $N$  within the measurement subinterval  $T$ :

$$\sigma_r^2 = \frac{\sigma_r^2}{N}, \quad \sigma_e^2 = \frac{\sigma_e^2}{N} \quad (13)$$

Standard measurement uncertainty of average value  $\bar{\Psi}$  is defined by standard deviation:

$$u(\bar{\Psi}) = \sqrt{\sigma_r^2 + \sigma_e^2} \quad (14)$$

The relative measurement uncertainty  $u$  is defined by the standard deviation and the average value of the accumulator output:

$$u = \frac{\sqrt{\sigma_r^2 + \sigma_e^2}}{\bar{\Psi}} \quad (15)$$

Similarly to [7] the standard measurement uncertainty and the relative measurement uncertainty are limited by:

$$u(\bar{\Psi}) \leq \frac{S_a \cdot (\sigma_n + \frac{\Delta_1}{2})}{\sqrt{N}}, \quad u \leq \frac{S_a \cdot (\sigma_n + \frac{\Delta_1}{2})}{\bar{\Psi} \cdot \sqrt{N}} \quad (16)$$

Limit of the standard measurement uncertainty (16) is determined by the root mean square (RMS) value of the auxiliary signal ( $S_a$ ), noise ( $\sigma_n$ ), the resolution in A/D converter ( $\Delta_1$ ), and by the number of samples within the measurement subinterval ( $N$ ). If  $R$  is the amplitude of the auxiliary signal, then:

$$S_a = R / \sqrt{2} \quad (17)$$

According to (10), (16) and (17) standard measurement uncertainty of any Fourier coefficient measured by this method is limited by:

$$u(a_k) = u(b_k) \leq \frac{\sqrt{2} \cdot (\sigma_n + \frac{\Delta_1}{2})}{\sqrt{N}} \quad (18)$$

$$u(\sqrt{a_k^2 + b_k^2}) \leq \frac{2 \cdot (\sigma_n + \frac{\Delta_1}{2})}{\sqrt{N}} \quad (19)$$

The quantum  $\Delta_1$  is defined by the A/D converter resolution, and the number of samples  $N$  can be a compromise between the necessary measurement speed and the required accuracy [7]. Therefore the system can have a very good accuracy even when the measurement noise is significant, due to the increased number of samples  $N$ .

If the A/D converter would be an ideal one, then  $\Delta_1=0$  and right side of (18) is transformed into  $\sqrt{2} \cdot \sigma_n / \sqrt{N}$ , which is square root of Cramér–Rao lower bound (CRLB) [12].

### III. MEASUREMENT EXAMPLE

As an example of non-stationary signal for testing the developed method, noisy brain potential is selected. These potentials are recordings of the small electrical potentials (generally less than 300  $\mu\text{V}$ ) produced by the brain [13-14]. They can be divided into two categories: spontaneous brain potentials, commonly named as EEG (electroencephalography) signals, and non-spontaneous brain potentials ERP (Event Related Potential) signals. The frequencies of spontaneous brain produced potentials range from 0.5 to 100 Hz, and their characteristics are highly dependent on the degree of activity of the cerebral cortex [15]. From a hardware standpoint brain potentials are the most difficult electrogram measurement to acquire [14].

The typical measurement system uses Ag/AgCl electrodes contained within a net or hat placed on the scalp of the patient; net or hat then connects to the hardware block using a cable several feet in length, subjecting the microvolt level brain potential to ambient noise that is many times greater than the signal itself. To amplify such low level voltage, this hardware block incorporates amplifying circuits but also Driven Right Leg (DRL) technique [16] and high-order analog filters with high gain (5000-20000 times) and sharp roll-off, to ensure that the only the desired signal is detected [17-18]. There are also some other techniques used for rejecting the noise, but they will be not be described here because it is out of the scope of this paper.

If implemented correctly, this conditioning of brain potential is generally satisfying. However, if the measurement system is exposed to high-level ambient noise (e.g. when brain potential measurements are combined with magnetic resonance imaging (MRI) where imaging artifacts appear and signal-to-noise ratio (SNR) can be extremely low), then this conditioning techniques are not satisfying (Fig. 7). In these cases it is necessary to apply some digital data processing for

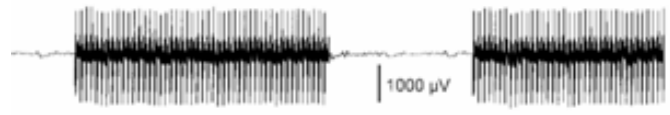


Fig. 7. The illustration from [22], showing the imaging artifact/noise in brain potential records during EEG/fMRI simultaneous recording (graph A). In this case, standard noise rejection techniques are not satisfying.

extracting brain potential [19-22].

### IV. SIMULATION

The aim of the simulation is to faithfully simulate previously described measurement system, in the case of measuring EEG signal. Hence, the simulation was implemented according to model from Fig. 3, and digital stochastic measurement block was implemented according to conceptual block-diagram from Fig. 6.

#### A. Input Signal and Conditioned Signal

Brain potential is chosen as an example of real non-stationary signal. Input signal is extracted from 2 seconds of real measurement session of the potential (Fig. 8). These values are amplified and superimposed with selected reference voltage (level transition and amplifying are usual tasks of conditioning brain potential), so the conditioned signal is actually the input of digital stochastic measurement block.

Real measurement was performed by the measurement system presented at Fig. 8. The amplifier is a three-stage amplifying and filtering circuit, implemented on one PCB (Printed Circuit Board). At the input, there is a electrostatic discharge protection circuit and passive low-pass filter for rejecting high frequencies (>1kHz).

First amplifying stage is a preamplifier based on instrumentation amplifier INA114P for obtaining high input impedance and high CMRR (Common Mode Rejection Ratio). Its amplification gain is 12. From this stage, inverted common mode voltage is driven to the DRL output of the amplifier and further to DRL cable and location of subject. This technique is often used when it is necessary to increase CMRR, and in this amplifier CMRR is 102dB.

Second amplifying stage has a central role for increasing the amplification gain (its gain is 40). Also, before input and

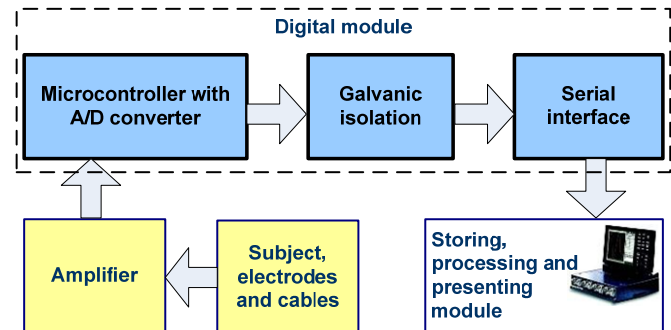


Fig. 8. System applied for real measurements. Amplifier is a three stage conditioning circuit. Digital module is consisted of microcontroller, digital optocouplers providing galvanic isolation and MAX232 providing serial interface to PC.

after output of this stage, there are high-pass filters with corner frequency of 0.15 Hz, thus providing rejection of offset voltage from amplifier input.

Third stage has role of final amplification (amplification is 16) and also of antialiasing filtering. The supply of the amplifier is unipolar (5 V), and there is also virtual ground buffered from 2 V voltage source. This voltage source is implemented on another PCB (the one with microcontroller) and leaded to the amplifier PCB.

Microcontroller module's main role is digitalization of the amplified voltage. This module is based on 8-bit microcontroller PIC18F4550 which has built-in A/D (analog-to-digital) converter with 10-bit resolution. Considering this resolution, the amplifier's amplification gain and A/D conversion reference voltage, the effective input resolution of the system is 0.5  $\mu$ V. Chosen sampling frequency of A/D conversion is 256 Hz. Digital outputs of microcontroller (RC6/TX and RC7/RX) are used for digital communication with PC based on UART (Universal asynchronous receiver/transmitter) protocol. Before connecting these outputs to MAX232 (digital chip for serial communication with PC), there are digital optocouplers implemented for achieving necessary galvanic isolation of the system.

Microcontroller is also connected with the input button, which is intended to be pressed by subject during specific cognitive tasks regarding recognition of stimuli.

In real measurement (which was a typical digital measurement), measurement records were stored 256 samples per second (S/s). For obtaining smooth simulation input and for adjusting simulation with experiment needs (described in the section dedicated to experiments) these 256 S/s records were transformed into 3,840 S/s data. This was achieved by 1) calculating Fourier coefficients by Discrete Fourier Transform (DFT) for original (256 S/s) records and 2) calculating

3,840 S/s data by using IDFT with previously calculated Fourier coefficients. Each sample of conditioned signal is stored as 64-bit floating point value in simulation lookup-table.

### B. Simulation Properties and Results

The DSMB was configured according to data presented in Table I. 4 sets of simulations was run – one without adding noise to the input signal, and other with adding white noise to the input signal. Noise has uniform Probability Density Function (PDF) and signal-to-noise ratio (SNR) was 10dB, 0dB and -10dB (Fig. 10). It is assumed there is no anti-aliasing filter before DSMB, which would limit the noise bandwidth. Therefore, comparing to classical design of conditioning block, it is worse situation (at first sight) regarding level of noise entering the digital block, but it is better situation regarding the size and optimization issues of conditioning block, because the number of conditioning block components are less.

For each SNR value, amplitude of harmonics determined by measured Fourier coefficients was compared versus amplitude determined by DFT of input signal, and absolute values of error was calculated (Table II and Fig. 11). The average error is compared versus theory maximum (19) in order to simplify comparison.

Also, the measured Fourier coefficients were used for calculating time-series (Fig. 12 shows the comparison when no noise is added). Peak-to-peak (pp) value of the resulting time-series is compared against the pp value of the input signal (Table III).

## V. EXPERIMENT

The aim of experiments was to test the theory maximum for measurement uncertainty and to compare experimental results against the simulation results.

TABLE I  
UNITS FOR MAGNETIC PROPERTIES

	<i>Simulations set 0</i>	<i>Simulations set 1</i>	<i>Simulations set 2</i>	<i>Simulations set 3</i>
<i>Number of simulations</i>	250	250	250	250
<i>SNR level</i>	No noise added	10dB	0dB	-10dB
<i>A/D converter (Fig. 6)</i>	Resolution: $m_1=6$ bits Input range: $\pm R$ and $R=2.5V$ Sampling frequency: $f_{adc} = 15625$ Hz			
<i>Measurement subinterval</i>	$[0, T]$ and $T = 20ms$			
<i>Fundamental frequency</i>	$f_0 = 1/T = 50Hz$			
<i>Number of samples per measurement subinterval</i>	$N = 312$			
<i>Digital dithered base functions</i>	Stored in memory in 64-bit floating point resolution but passed to the multiplier in 8-bit resolution, thus faithfully simulating an A/D converter with properties: Resolution: $m_2 = 8$ bits Range: $\pm R$ and $R=2.5V$ Sampling frequency: $f_{adc} = 15625$ Hz			
<i>Number of measured Fourier coefficients</i>	DC component + 15 sine coefficients + 15 cosine coefficients			

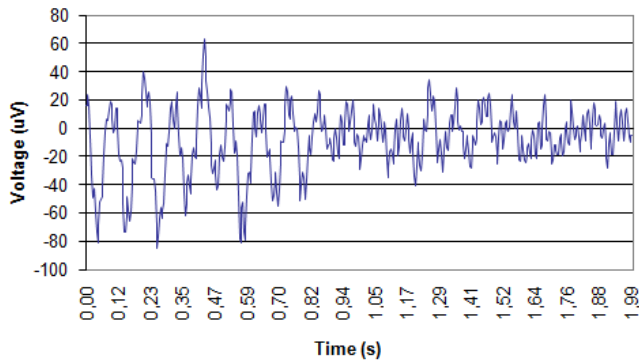


Fig. 9. 2 seconds of recording brain potential. This signal was used for both simulation and experiment input.

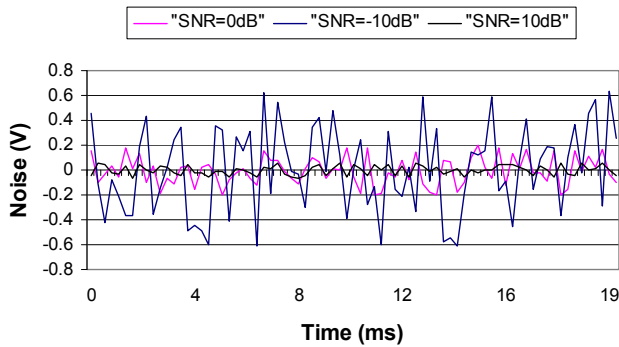


Fig. 10. The examples of the noise added to the input signal of simulations, for various SNR levels. The noise is generated (in both simulation and experiment) at rate of 3840 samples per second.

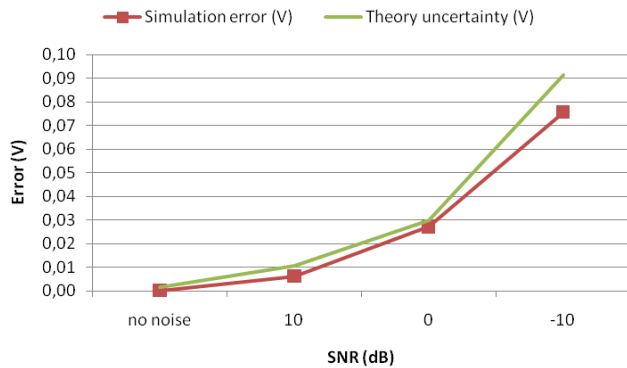


Fig. 11. Average error per harmonic compared against theory maximum for measurement uncertainty.

### A. Input Signal

The plan of experiments required 4 sets of experiments (actually  $4 \cdot 250 = 1000$  experiments) as the simulations were consisted of 4 sets of simulations. For obtaining correct results, comparable with theory and simulation, each experiment had to measure the same signal. Of course, this repeatability of brain potential could not be achieved with humane subject and “live” measurement for each experiment.

Therefore, the source of signal in experimental measurements was not the humane subject, but an artificial source of conditioned signal was made. The same data for conditioned brain potential at the input of DSMB, used in

TABLE II

SIMULATION AVERAGE ERROR PER HARMONIC COMPARED AGAINST THEORY MAXIMUM FOR MEASUREMENT UNCERTAINTY (19)				
SNR (dB)	no noise	10	0	-10
Simulation error (V)	2,08E-04	6,29E-03	2,72E-02	7,57E-02
Theory uncertainty (V)	1,41E-03	1,05E-02	3,00E-02	9,16E-02

TABLE III

RELATIVE ERRORS FOR PEAK-TO-PEAK VALUE AT VARIOUS SNR LEVELS				
SNR (dB)	no noise	10	0	-10
Peak-to-peak relative error (%)	0.26	2.67	46.19	268.69

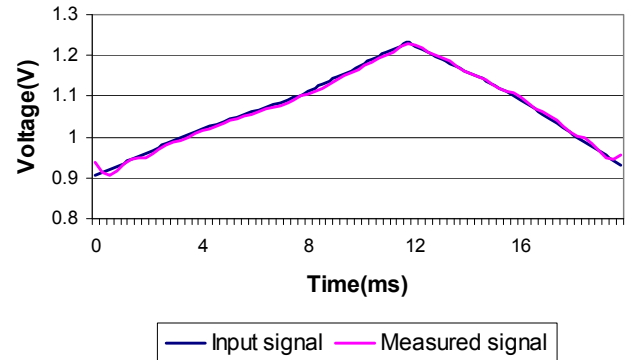


Fig. 12. Comparison of input signal and measured signal in simulations set 0. Measured signal is reconstructed by measured Fourier coefficients. Measurement subinterval is [0, 20ms] and noise is not added to the input signal.

simulations, were also used for the artificial source to generate the signal.

This source was made by development board with a programmable system-on-chip (PSoC) CY8C27843 (Fig. 13), using an embedded 8-bit digital-to-analog (D/A) converter, 16-bit counter and lookup table. Digital values, calculated from brain potential measurement results before experiment, were stored in lookup table (actually 4 sets of digital values depending on SNR level), and sample rate was configured to be 3,840 Hz which provides relatively smooth analog signal at the output. The configured range of D/A converter is from 0 V to 2.6 V.

### B. Implementation of DSMB

At first sight, block diagram from Fig. 6 seems to require complex hardware structure but its hardware implementation can be relatively simple. Block diagram of the hardware implementation is given at Fig. 14, and the photos of hardware at Fig. 15. This hardware implementation was originally developed for measuring line voltage and current harmonics.

The multipliers and accumulators are implemented by FPGA structure (chip Cypress CY39100) which finally calculates Fourier coefficients. The microprocessor (Atmel AT89s8252) interfaces the block with PC, i.e. interfaces FPGA chip with PC. Pseudostochastic dither signal is generated by FPGA chip and analog adder is required for performing addition of dither. The memory is flash EEPROM

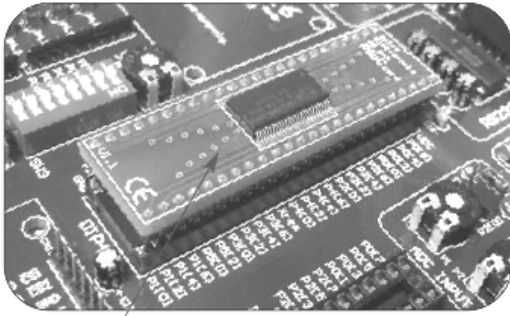


Fig. 13. PSoC CY8C27843 (its mounting on the development board is pointed by arrow) is used as the generator of conditioned signal.

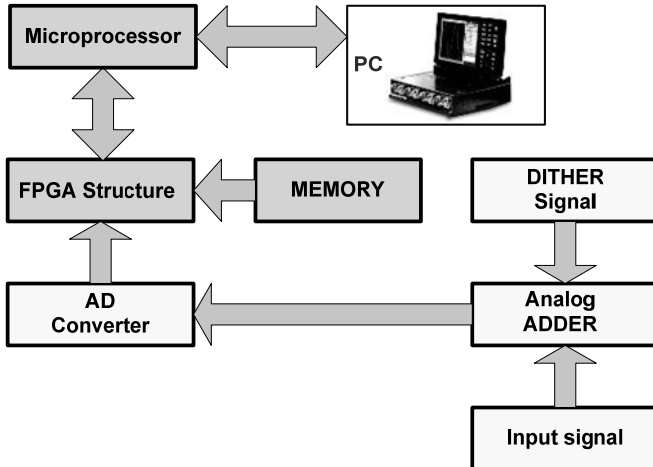


Fig 14. Hardware block diagram of digital stochastic measurement block interfaced to PC.

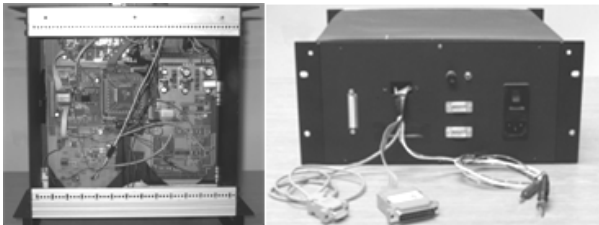


Fig 15. Prototype hardware implementation of block diagram from Fig 13.

memory M29F040 with capacity of 512 Kb.

A/D converter's properties are the same as in simulations (resolution:  $m_1=6$  bits, input range:  $\pm 2.5$  V, sampling rate:  $f_{adc}=15,625$  Hz). Regarding A/D converter, an important thing is that this A/D converter can generally have lower resolution and faster conversion time than the one in typical digital measurement, which can be useful for parallelization of measurements necessary for multichannel recordings.

FPGA chip is programmed with a very-high-speed integrated circuits hardware description language (VHDL) program. The VHDL program is consisted of 4 processes (P1, P2, P3 and P4) which execute simultaneously. Process P1 receives 6-bit digital values from A/D converter. Process P2 is the main process, and all the mathematical calculations are implemented by this process. Process P3 has the task to send the results of process P2 to the microprocessor. Process P4 waits for request from the microprocessor, and when the request comes in P4 activates the process P3.

TABLE IV  
AVERAGE ERROR PER HARMONIC COMPARED VERSUS THEORY MAXIMUM FOR MEASUREMENT UNCERTAINTY (19)

SNR (dB)	no noise	10	0	-10
<i>Experiment error (V)</i>	2,51E-04	7,73E-03	2,77E-02	7,95E-02
<i>Simulation error (V)</i>	2,08E-04	6,29E-03	2,72E-02	7,57E-02
<i>Theory uncertainty (V)</i>	1,41E-03	1,05E-02	3,00E-02	9,16E-02

PC software application receives the data from microprocessor, records and presents the measurement results.

### C. Results

4 sets of experiments were done in the same way as simulations – one without adding noise to the input signal, and other with adding white noise (Fig. 10) to the input signal. Noise has uniform PDF and signal-to-noise ratio (SNR) was 10 dB, 0 dB and -10 dB.

For each SNR value, amplitude of harmonics determined by measured Fourier coefficients was compared versus amplitude determined by DFT of input signal data, and absolute values of error was calculated (Table IV and Fig. 16).

Experiment results showed well adjustment with the limits calculated by formula (19) for three SNR values (10 dB, 0 dB and -10 dB). Resolution of the D/A converter used for generating input signal, and the ambient noise interfered with the interface between input signal generator and DSMB are recognized as factors responsible for the fact that experimental errors are higher than simulation errors.

## VI. DISCUSSION

Hardware resources used in implementation of the digital stochastic measurement block (Fig. 14 and Fig. 15) are pretty modest comparing to the technology state of the art. In future research, it would be interesting to investigate, what would be the results of measurement if the sampling frequency of the A/D converter is drastically increased (e.g. 1 MHz) and if the number of measured harmonics is increased, because actual A/D and FPGA chips allow such implementation and theoretically developed formula for measurement uncertainty limit indicates the possibility of significant improvement of the measuring system accuracy and noise rejection.

It would also be interesting to extend measurement subinterval (e.g. to 2, 4 or 8 seconds, because FFT of brain potential is usually calculated for a short section of time series - from 1 to 8 seconds [13]). This extension would increase the number of samples involved in measurement subinterval (i.e. increase the accuracy), but it would also increase delay time for presenting reconstructed time-series. This delay time would be disadvantage if the application of measurement would include necessity for real-time control/reaction, but otherwise this would not be problematic (like in measurements of ERP brain potential, when processing of measurement data is performed after the appropriate measurement interval [23]).

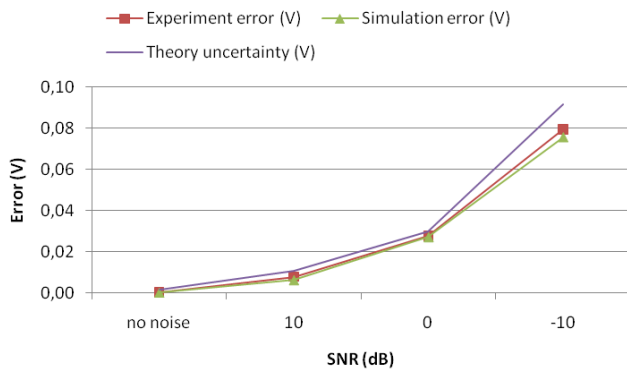


Fig 16. Average error per harmonic by experiment compared against simulation results and theory maximum for measurement uncertainty.

## VII. CONCLUSION

Accurate measurement of weak and noisy signals presents a challenge in digital measurements. The previous research on digital stochastic measurement shown to be relatively robust to noise as it gives accurate results even when the noise is greater than the measured stationary signal.

The research described in this paper evaluated digital stochastic measurement method implementation for non-stationary signals and compared it to the method implementation for stationary signals. Developed theory resulted in formula for theory limit of measurement uncertainty, and this theory is tested with applied simulations and experiments.

Brain potential is chosen as an example of real non-stationary signal which is to be measured. The noise is added in three sets of simulations and experiments for inspecting the noise rejection of the method.

The experimental test signal generator and prototype instrument has been used in experiments. The implemented digital stochastic measurement block includes a flash A/D converter, a memory for dithered base functions, and one signal multiplier and a digital accumulator for each sine and cosine components of the measured harmonics realized by FPGA structure.

The simulations and experiments have shown well agreement with the developed formula for measurement uncertainty limit. This formula shows the possibility of controlling measurement uncertainty even if it is necessary to work with the constant measurement subinterval. This limit is dependent on number of samples over the measurement interval, which is determined by sampling rate of A/D converter inside digital stochastic measurement block, allowing designer to choose A/D converter with lower resolutions and faster sampling rate for achieving more accurate measurement and measurement more robust to noise.

## REFERENCES

- [1] M.B. Priestley, *Non-linear and Non-stationary Time Series Analysis*, Academic Press, 1988.
- [2] W. J. Fitzgerald, R. L. Smith, A. T. Walde, P. C. Young, *Nonlinear and Nonstationary Signal Processing*, Cambridge University Press; 1st ed, 2001.
- [3] J. von Neumann, "Probabilistic logic and the synthesis of reliable organisms from unreliable components," in *Automata studies*, CE Shannon, Ed. Princeton, NJ: Princeton University Press, 1956.
- [4] M.F.Wagdy, W.Ng, "Validity of uniform quantization error model for sinusoidal signals without and with dither," *IEEE Trans. Instrum. Meas.*, vol. 38, pp. 718-722, June 1989.
- [5] V. Vujičić, S. Milovančev, M. Pešaljević, D. Pejić and I. Župunski, "Low frequency stochastic true RMS instrument," *IEEE Trans. Instrum. Meas.*, vol. 48, pp.467-470, Apr. 1999.
- [6] D. Pejić, V. Vujicic, "Accuracy limit of high-precision stochastic Watt-hour meter," *IEEE Trans. Instrum. Meas.*, vol. 49, pp. 617-620, June 2000.
- [7] B. Santrač, M. A. Sokola, Z. Mitrović, Ivan Župunski and V. Vujičić, "A Novel Method for Stochastic Measurement of Harmonics at Low Signal-to-Noise Ratio", *IEEE Trans. Instrum. Meas.*, vol. 58, pp. 3434-3441, Oct. 2009.
- [8] V. Pjevalica, and V. Vujičić, "Further Generalization of the Low-Frequency True-RMS instrument (Periodical style—Accepted for publication)", *IEEE Trans. Instrum. Meas.*, to be published.
- [9] Sovilj P. M., Milovančev S. S., Vujičić V.: Digital Stochastic Measurement of a Nonstationary Signal With an Example of EEG Signal Measurement, *Instrumentation and Measurement IEEE Transactions on*, Vol. 60 - issue 9, pp. 3230-3232, 2011.
- [10] V. Vujičić, "Generalized low frequency stochastic true RMS instrument", *IEEE Trans. Instrum. Meas.*, vol. 50, pp. 1089-1092, Oct. 2001.
- [11] A. Papoulis, "Probability, random variables and stochastic processes", McGraw-Hill series in Systems Science, USA, 1965.
- [12] S.M. Kay, "Fundamentals of Statistical Signal Processing, Volume I: Estimation Theory", Vol. I, 1st ed., pp. 27-82, New Jersey: Prentice Hall PTR, 1993.
- [13] J.D. Bronzino, "Principles of Electroencephalography", in *Biomedical Engineering Handbook*, Vol. I, J.D. Bronzino, 2nd ed., New York: CRC Press LLC, 2000.
- [14] J. G. Webster, "Medical Instrumentation Application and Design", New York: Wiley, 1998.
- [15] M. Abeles and M. Goldstein, "Multispikes Train Analysis", *Proc. IEEE*, No. 65, pp (762-773), 1977.
- [16] B. B. Winter and J. G. Webster, "Driven-right-leg circuit design", *IEEE Trans. Biomed. Eng.*, vol. 30, pp. 62-66, 1983.
- [17] M. Kutz, "Standard Handbook of Biomedical Engineering and Design", McGraw-Hill, 2003.
- [18] B. A. Schmitz, "Improving signal quality and test reliability in EEG measurements using integrated high-density surface-mount electronics", *SMAT Medical Electronics Symposium*, Minneapolis Airport Marriott, Bloomington, May 2004
- [19] L. M. Angeloneb, P. L. Purdona, J. Ahveninena, J. W. Belliveaua and G. Bonmassara, "EEG/(f)MRI measurements at 7 Tesla using a new EEG cap ("InkCap")", *NeuroImage*, vol. 33, pp. 1082-1092, 2006
- [20] M. Negishi, B.I. Pinus, A.B. Pinus and R.T. Constable, "Origin of the Radio Frequency Pulse Artifact in Simultaneous EEG-fMRI Recording: Rectification at the Carbon-Metal Interface", *IEEE Trans. Biomed. Eng.*, Sept. 2007, vol. 54, pp. 1725 - 1727
- [21] S. M. Mirsattari, J. R. Ives, S. Leung and R. S. Menon, "EEG Monitoring during Functional MRI in Animal Models", *Epilepsia*, vol. 48(suppl. 4), pp. 37-46, Blackwell Publishing, Inc., 2007
- [22] Philip J. Allen, Oliver Josephs, and Robert Turner, "A Method for Removing Imaging Artifact from Continuous EEG Recorded during Functional MRI", *NeuroImage*, vol. 12, pp. 230-239, 2000
- [23] E. Donchin, K. M. Spencer, and R. Wijesinghe, "The mental prosthesis: Assessing the speed of a P300-based brain-computer interface," *IEEE Trans. Rehab. Eng.*, vol. 8, pp. 174-179, June 2000.